Experimental and Theoretical Investigation of 1,1,2,3,3-Pentamethylenepropane Model Systems

Mark L. Kearley,† Andrew S. Ichimura, and Paul M. Lahti*

Contribution from the Department of Chemistry, University of Massachusetts, Amherst, Massachusetts 01003-4510

Received January 3, 1995®

Abstract: Pyrolysis and photolysis of derivatives of 2,4-dibenzylidenebicyclo[3.1.0]hexan-3-one cause isomerization at the cyclopropyl ring, consistent with formation of a pentamethylenepropane (PMP)-type intermediate or transition state. Kinetic studies of the isomerization gave E_a = 31 kcal/mol and log(A) = 11.2, consistent with reasonable thermodynamic estimates for the formation of a PMP-type species. No evidence was found under rigid cryogenic conditions for a triplet PMP in photolysis of the bicyclo[3.1.0]hexan-3-ones. Computational studies indicate that bicyclic PMP derivatives 1,2,3-trimethylenecyclohexane-4,6-diyl and 2,6-dimethylenecyclohexanone-3,5-diyl have $^3B_2$ ground states, by <2 kcal/mol relative to their respective diradical $^1A_1$ states. This close spacing of the singlet and triplet energy manifolds is probably in part responsible for the ineffectiveness of generation of the triplet PMPs from singlet bicyclo[3.1.0]hexan-3-one precursors.

Introduction

Among questions of interest to workers investigating organic π-conjugated diradicals and polyradicals, the disjoint class of non-Kekulé molecules has been a salient problem.[1] Borden and Davidson originally described[2] the disjoint classification scheme and made the prediction that these diradicals should possess unusually small energy gaps between triplet and singlet states. Since then, a number of disjoint non-Kekulé molecules have been the subjects of computational and experimental work. For example, the tetramethyleneethane (TME, **1**) system has been intensively studied. It is an archetypal disjoint system that experimentally has been shown to be a ground state triplet diradical,[3,4] but which was computationally predicted to be a ground state singlet[5−7] until recent computations[8] showed that geometric distortions *can* lead to a triplet TME ground state.

A particularly intriguing member of the disjoint class is 1,1,2,3,3-pentamethylenepropane (PMP, **2**) and its analogues. PMP and systems related to it have the interesting distinction of being disjoint by the Borden/Davidson classification,[2] but being predicted by other qualitative connectivity-based schemes to be a high-spin triplet ground state diradical.

Semiempirical molecular orbital plus configuration interaction computations suggest that PMP would be a ground state triplet diradical, in accord with parity-based qualitative models.[9,10] No direct experimental test of this prediction is available for PMP itself. However, recent experimental studies[11,12] of conjugated bis(arylnitrene) systems **3**—which are connectivity analogues of PMP, as we shall further discuss below—have been found to have low-spin ground states, in qualitative agreement with the disjointness criterion. As a result, PMP remains a system whose electronic nature and ground state spin multiplicity remain unclear. In this contribution, we give full details of an isomerization study of a geometrically constrained PMP precursor system, 2,4-dibenzylidene-bicyclo[3.1.0]hexan-3-one (**4**).[13] We also describe computational studies of the experimentally plausible PMP derivatives 1,2,3-trimethylenecyclohexane-4,6-diyl (**5**) and 2,6-dimethylenecyclohexanone-3,5-diyl (**6**).

Chart 1

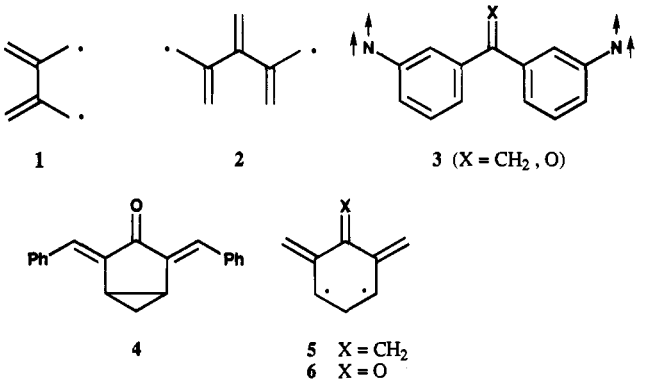

1 **2** **3** (X = CH_2, O) **4** **5** X = CH_2 **6** X = O

General Procedures

Synthesis. Figure 1 shows the syntheses of bicyclic PMP precursors **4** and **7**. Standard literature methods were used to make cyclopenten-4-ol,[14] which was cyclopropanated by the method of Nishimura *et al.*[15] to give the desired bicyclo[3.1.0]hexan-3-ol **8** or **9**. ^{1}H NMR

†Present address: Department of Chemistry, Creighton University, Omaha, NE 68178-0104.

® Abstract published in *Advance ACS Abstracts,* April 15, 1995.

(1) Cf.: *Diradicals*; Borden, W. T., Ed.; John Wiley and Sons, Inc.: New York, 1982.
(2) Borden, W. T.; Davidson, E. R. *J. Am. Chem. Soc.* **1977**, *99*, 4587.
(3) Dowd, P.; Chang, W.; Paik, Y. H. *J. Am. Chem. Soc.* **1986**, *108*, 7416.
(4) Dowd, P.; Chiang, W.; Paik, Y. H. *J. Am. Chem. Soc.* **1987**, *109*, 5284.
(5) Du, P.; Hrovat, D. A.; Borden, W. T. *J. Am. Chem. Soc.* **1986**, *108*, 8086.
(6) Du, P.; Borden, W. T. *J. Am. Chem. Soc.* **1987**, *109*, 930.
(7) Nachtigall, P.; Jordan, K. D. *J. Am. Chem. Soc.* **1992**, *114*, 4743.
(8) Nachtigall, P.; Jordan, K. D. *J. Am. Chem. Soc.* **1993**, *115*, 270.
(9) Lahti, P. M.; Rossi, A. R.; Berson, J. A. *J. Am. Chem. Soc.* **1985**, *107*, 2273.
(10) Lahti, P. M.; Ichimura, A. S.; Berson, J. A. *J. Org. Chem.* **1989**, *54*, 958.
(11) Ling, C.; Minato, M.; Lahti, P. M.; van Willigen, H. *J. Am. Chem. Soc.* **1992**, *114*, 9959.
(12) Matsumoto, T.; Ishida, T.; Koga, N.; Iwamura, H. *J. Am. Chem. Soc.* **1992**, *114*, 9952.
(13) A preliminary report of portions of this work appeared in the following: Kearley, M. L.; Lahti, P. M. *Tetrahedron Lett.* **1991**, *32*, 5869.
(14) Hess, H. M.; Brown, H. C. *J. Org. Chem.* **1967**, *15*, 70.
(15) Nishimura, J.; Kawabata, N.; Furukawa, J. *Tetrahedron* **1969**, 25, 2647.

0002-7863/95/1517-5235$09.00/0

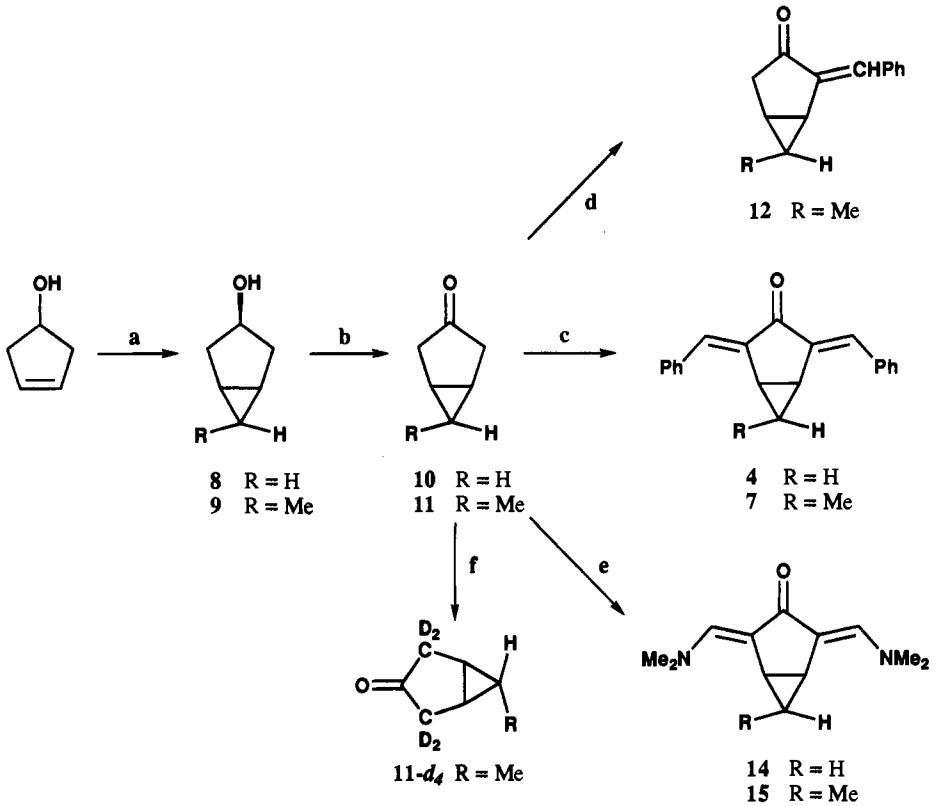

Figure 1. Syntheses for bicyclic PMP precursors. (a) Et_2Zn/hexanes/Et_2O/ $RCHI_2$. (b) Pyridinium dichromate/CH_2Cl_2. (c) PhCHO (3 equiv)/ EtOH/NaOH. (d) PhCHO (0.5 equiv)/EtOH/NaOH. (e) $Me_2CH(O^tBu)_2$/90 °C. (f) MeOD/MeONa/D_2O.

Chart 2

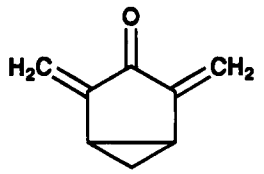

13

spectroscopy showed the ethylidenation product **9** to have the 6-methyl group almost exclusively in the *exo* position, by using the spectral structure assignments previously obtained by Nishimura *et al.* The alcohols **8** and **9** were readily oxidized by pyridinium dichromate to ketones **10** and **11** and subjected to aldol double benzylidenation to give the PMP precursors **4** and **7**. The benzylidene groups in **4** and **7** were assigned the *E*-geometry, since vinyl protons in geometrically related molecules appear at δ 7.6 ppm, while those of related *Z*-exocyclic benzylidene compounds appear at δ 6.8 ppm;[16] our compounds have vinyl singlets at ca. δ 7.9 ppm. In addition, the benzylidenation of **11** could be stopped after a single step to give compound **12**, which we used for control studies to be described below.

Efforts to make methylenated model compounds such as **13** by the method of Gras[17] (paraformaldehyde/*N*-methylanilinium trifluoroacetate) were not promising. Although some of the desired product **13** could be generated from cyclopentanone according to ^{1}H NMR and GC analysis of the crude reaction mixture, this compound readily polymerized during workup. We therefore avoided unsubstituted methylenation reactions. Condensation of **10** or **11** with *N*,*N*-dimethylformamide di-*tert*-butyl acetal gave 2,4-bis[(*N*,*N*-dimethylamino)methylene]bicyclo[3.1.0]hexan-3-one derivatives **14** and **15**. These compounds were assigned the *E*-stereochemistry at the exocyclic benzylidene groups and the *exo*-configuration at the 6-methyl position, based on NMR arguments analogous to that described above. Further functionalization of **14** and **15** is possible,[18] but we chose to limit our study to this set of derivatives.

Computational Methods. Geometry optimizations were carried out using GAMESS,[19] GAUSSIAN88, and GAUSSIAN92.[20] GAMESS was implemented on a Celerity 1260D UNIX minicomputer and a Silicon Graphics Indigo R4000 workstation, GAUSSIAN88 was implemented on the Cornell National Supercomputer Facility IBM computer, and GAUSSIAN92 was implemented on the University of Massachusetts Computer Services DEC VAX system. For SCF computations on **5** and **6**, the $^3B_2$ state was optimized with the 6-31G* basis set using an unrestricted Hartree–Fock (UHF) wave function. The $^1A_1$ state was optimized with the same basis set using a two-configuration self-consistent field (TCSCF) wave function. All geometries were optimized to a tolerance of less than 1 millihartree/ bohr. Frequency analysis of the $^3B_2$ UHF and $^1A_1$ TCSCF 6-31G* stationary points showed them to be energy minima.

Configuration interaction (CI) computations were carried out at fixed geometries, using the MELDF[21] suite of programs developed by Davidson and co-workers. For $^3B_2$ CI calculations, 6-31G*-restricted open-shell Hartree–Fock (ROHF) molecular orbitals (MOs) were used with varying configuration generation schemes. Some computations were performed at the singles plus doubles level (SD-CI) within a limited active subspace of the SCF MOs. Larger computations at a level up to quadruple excitations (SDTQ-CI) were also carried out. The active spaces used in these CI computations are described in the

(16) George, H.; Roth, H. J. *Tetrahedron Lett.* **1971**, 4057.
(17) Gras, J.-L. *Tetrahedron Lett.* **1978**, 2111.
(18) To replace the dialkylamino groups with methyl groups to get bis-(ethylidene) deriviatives, cf.: Blaustein, M. Ph.D. Thesis, Yale University, New Haven, CT, 1983.
(19) Schmidt, M. M.; Baldridge, K. K.; Boatz, J. A.; Jensen, J. H.; Koseki, S.; Gordon, M. S.; Nguyen, K. A.; Windus, T. L.; Elbert, S. T. *QCPE Bull.* **1990**, *10*, 52.
(20) Frisch, M. J.; Trucks, G. W.; Schlegel, H. B.; Gill, P. M. W.; Johnson, B. G.; Wong, M. W.; Foresman, J. B.; Robb, M. A.; Head-Gordon, M.; Replogle, E. S.; Gomperts, R.; Andres, J. L.; Raghavachari, K.; Binkley, J. S.; Gonzalez, C.; Martin, R. L.; Fox, D. J.; Defrees, D. J.; Baker, J.; Stewart, J. J. P.; Pople, J. A. *Gaussian 92/DFT*, Revision G.2; Gaussian, Inc.: Pittsburgh, PA, 1993.
(21) Developed at the University of Washington by L. McMurchie, S. Elbert, S. Langhoff, and E. R. Davidson and modified by D. Feller and D. Rawlings.
(22) Feller, D.; Davidson, E. R. *J. Chem. Phys.* **1981**, *74*, 3977.

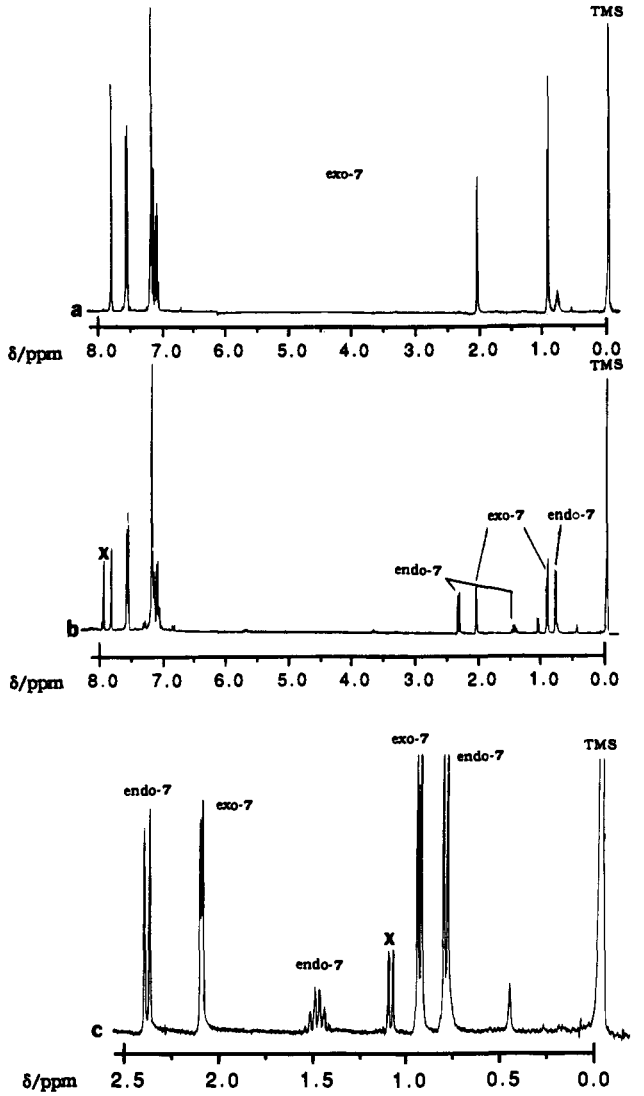

Figure 2. ^{1}H NMR of **7** before and after epimerization. (a) 300 MHz ^{1}H NMR spectrum of *endo*-**7** in C_6D_6. (b) 300 MHz ^{1}H NMR spectrum of *endo*-**7** after photolysis at 254 nm at room temperature. **X** marks peaks due to product from isomerization of the exocyclic benzylidene (=CHPh) group, which are not observed in thermal isomerizations. (c) Abscissa expansion of spectrum b at 300 MHz, δ 0.0–2.5 ppm.

Results below. In all cases, the virtual orbital subspaces were transformed into K-orbitals[22] to improve the recovery of correlation energy.

Results

Photolysis of Bicyclic PMP Precursors. All of the PMP precursors **4**, **7**, **14**, and **15** are yellow solids with strong absorption maxima in the 300–400 nm region of the UV–vis spectrum. Photolysis of precursors **4** and **14** in benzene-d_6 or nitrobenzene-d_5 at 254 nm or 350 nm at 25 °C through pyrex gave no significant changes in the ^{1}H NMR spectrum. At long irradiation times we observed growth of small resonances in the vinylic region (δ 6.5–7.0 ppm). We attribute these vinylic resonances to products where the cyclopropane ring was cleaved.

Solution photolysis of methyl-labeled precursor **7** showed appreciable changes in the ^{1}H NMR spectrum (Figure 2). Some isomerization about the exocyclic benzylidene groups was indicated by the production of a new peak in the δ 6.8–8.1 ppm (=C*H*Ph) region, with an intensity-associated peak at δ 1.1 ppm (d, CH_3). In addition, *exo* to *endo* isomerization occurred at the 6-methyl position. In C_6D_6, this isomerization was observable by (1) the production of a new *endo* methyl doublet (δ 0.82 ppm, J = 6.6 Hz) which is upfield of the *exo* methyl doublet (δ 0.95 ppm, J = 6.1 Hz); (2) a new multiplet due to the *endo* C_6–H (δ 1.46) which is downfield of the multiplet for the original *exo* C_6–H (δ0.80); and (3) a new doublet (δ2.34, J = 8.3 Hz) due to the bridgehead hydrogens which is downfield of the bridgehead resonances in the *exo* isomer (δ 2.06 ppm, d, J = 3.4 Hz). Stereochemical assignments are based on Nishimura's[15] previous work. Presumably, C_6 epimerization also occurs in **4** but is unobservable due to the lack of a substituent label. This isomerization was not observed for the bis(enamine) derivative **15** under photochemical conditions attempted by us, possibly due to the efficient fluorescence observed in **14** and **15** (see below).

Chart 3

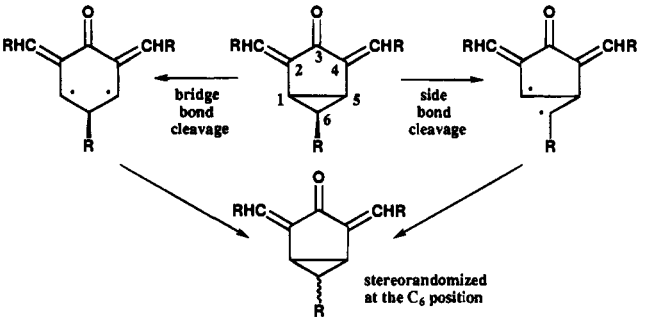

These data indicate that solution phase isomerization—consistent with PMP formation—occurs in precursor **7**. However, it is also possible that side bond cleavage occurs instead of or in competition with cleavage of the bridge bond, leading to the observed isomerization. We tested for this possibility by looking for evidence of side bond cleavage in model compounds that cannot form PMPs. Photolysis of the bicyclic model ketone **11**-*2,2,4,4-d*$_4$ showed no changes by ^{1}H NMR under the same conditions used for **7**. However, extended photolysis of the monobenzylidenated compound **12** suggested some cyclopropane epimerization, shown by production of a new methyl doublet upfield of that in the original reactant. As a result, some amount of side-bond cleavage may be involved in photochemical epimerization of **7**.

We attempted to observe the ESR or UV–vis spectra of a diradical intermediate in the frozen solution photolysis of **4** (2-methyltetrahydrofuran, 77 K, pyrex-filtered 1000 W xenon arc). Under no conditions did we observe any spectral changes attributable to a diradical. Variations on the photolysis procedure included addition of triplet sensitizers and continuous photolysis while in the ESR cavity. Control experiments showed that 77 K frozen solution photolysis of **7** of the same duration used in room temperature fluid solution photolysis did *not* lead to isomerization at C_6, ruling out possible formation of a planar PMP under these conditions. This surprising and disappointing result may be due to depopulation of the photochemically excited state through photophysical processes (described later) that compete effectively under rigid phase conditions with photochemical bond cleavage. This lack of rigid phase isomerization may well be the reason for our failure to observe any ESR spectral peaks that could be assigned to PMP derivatives during the photolysis of bicyclic precursors **4** and **7**.

Thermolysis of Bicyclic PMP Precursors. Thermolysis of precursor **4** showed no changes in the ^{1}H NMR spectrum at temperatures of up to 210 °C for at least 60 min. But, similar thermolyses of *exo*-**7** gave a nearly 1:1 mixture of *exo* and *endo* isomers. Unlike the case of photochemical isomerization, there was no evidence in the ^{1}H NMR spectrum of isomerization at the exocyclic benzylidene groups (peaks "X" in Figure 2).

Chart 4

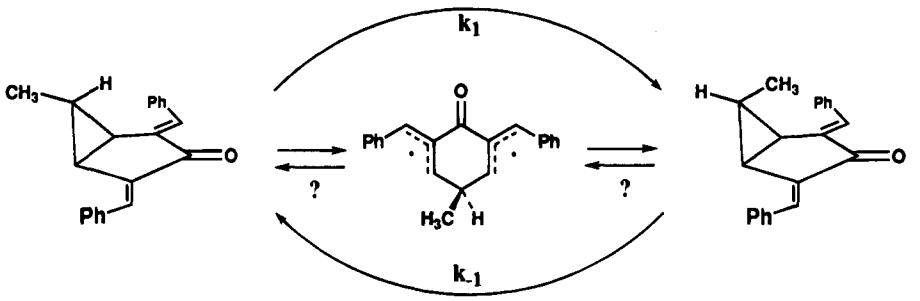

Table 1. Equilibrium Data and Rate Constants k_1 for *exo* → *endo* Epimerization of **7** in $C_6D_5NO_2$ at Various Temperatures

temp/°C	initial [*exo*-**7**]/M	final [*endo*-**7**]/M	K_{eq} (calcd)	$\Delta G_{eq}°$/ kcal/mol	$10^5k_1/s^{-1}$
164.3	0.192	0.050	0.35	0.91	5.4
174.5	0.192	0.054	0.39	0.84	11.7
185.1	0.192	0.054	0.39	0.86	28.3
195.1	0.164	0.048	0.41	0.83	57.2
204.5	0.164	0.044	0.37	0.94	113.0

By monitoring the rate of production of *endo*-**7**, we carried out ^{1}H NMR kinetic experiments on the epimerization process over the temperature range 164.3−204.5 °C in nitrobenzene-d_5, using eq 1, which is applicable for a reversible one-step

$$d[x]/dt = k_1x_0/([x]_e([x]_e - [x]) \quad (1)$$

reaction.[23] In eq 1, x_0 is the starting concentration of *exo*-**7**, x_e is the equilibrium concentration of *endo*-**7** determined by letting a control reaction continue overnight at each temperature, while k_1 is the forward reaction from *exo* to *endo*-**7**. We assumed simple equilibration of *exo*- and *endo*-**7** without side reactions and so could directly relate ^{1}H NMR integration values to the known starting concentration x_0 of *exo*-**7** in each experiment. Table 1 shows the equilibrium constants K_{eq} = [*endo*-**7**]/[*exo*-**7**] obtained by measuring [x_e] at long reaction times for various temperatures, as well as the associated ΔG(*endo*−*exo*) in each case; epimerization rate constants k_1 are also shown, using eq 1. Figure 3 summarizes the kinetic data. In all cases, the rate constants were obtained by statistically weighted linear least squares, with all correlation coefficients found to be >0.996. The rate constant data yielded Arrhenius kinetic parameters of E_a = 31.0 ± 0.5 kcal/mol and log(A) = 11.2 ± 0.3 and Eyring kinetic parameters of $\Delta H^‡$ = 29.8 ± 0.5 kcal/mol and $\Delta S^‡$ = −10.8 ± 1.1 cal/(mol-deg); the uncertainties are standard deviations.

We also investigated the possibility of wrong-bond cleavage as a major contributor to thermal epimerization of **7**. Prolonged thermolyses of model compounds **11**-2,2,4,4-d_4 and **12** showed no sign by ^{1}H NMR of epimerization at the C_6 position. Thus, so far as we can deduce, the thermal epimerization of **7** (unlike the photolytic epimerization) requires the presence of both α-benzylidene groups, consistent with production of a PMP-type intermediate or transition state in this process.

As in the attempted photolytic analogue reaction, thermolysis of bis(enamine)-substituted PMP precursor **15** gave no epimerization visible by ^{1}H NMR, but merely solution discoloration consistent with minor amounts of decomposition.

Choice of PMP Computational Wave Functions. Using the 6-31G* UHF-SCF $^3B_2$ geometries of **5** and **6** as starting guesses, we carried out a series of computations aimed at finding whether the $^3B_2-{}^1A_1$ state energy gap was sensitive to a choice of CI wave function. We used SDTQ-CI wave functions with varying inclusion of p-space orbitals. We also used SD-CI wave functions with both π and σ orbitals in the active space; in these computations, a two-configuration reference state was used for the $^1A_1$ computations (σ,π-MRSD-CI level), while a single configuration reference state was used for the $^3B_2$ state. In addition, we made estimated corrections to the SD-CI level results for the effect of quadruple excitations (SDQ-CI).[24] These various results are summarized in Table 2.

The SCF/TCSCF level results show a slight favoring of the $^3B_2$ states at a fixed geometry. The preference increases to about 1−2 kcal/mol for **5** and **6** at both the SDTQ-CI and MRSDQ-CI levels of theory. Increasing the number of p-orbitals retained in the active space of π-SDTQ-CI computations did not appreciably alter the results, as exemplified for **5** in Table 2. Neither did the use of enlarged orbital active spaces in a σ,π-MRSD-CI level of approximation change results much relative to the π-SDTQ-CI results for heteroatom-containing **6**. In both **5** and **6**, it appears that $\sigma-\pi$ orbital subspace separability may be used without serious detriment to the computational results, as was observed in earlier work[25] on the diradical *m*-benzoquinodimethane.

These results suggested that a choice of CI wave function would not be too sensitive an issue in computations of $\Delta E(T-S)$ for **5** and **6**. We decided to use an SDTQ-CI wave function for partial CI geometry optimizations described below, with excitation of all π electrons within a 12 π-orbital subspace: no orbitals of σ symmetry were included. This choice allowed fairly quick computation of SDTQ-CI energies at different geometries, but without serious loss of precision in describing the PMP $^3B_2-{}^1A_1$ energy gaps, to judge by the results of Table 2.

Computational Analysis of PMP Geometric Structure. The SCF level 6-31G* geometries found for **5** were qualitatively quite different for the UHF $^3B_2$ and TCSCF $^1A_1$ states, as shown in Figure 4. While the UHF geometry has the delocalized "bis-(allyl)"-type structure expected of PMP, the TCSCF geometry was substantially localized. SDTQ-CI computations at these fixed geometries found the localized TCSCF structure to give lower $^3B_2$ and $^1A_1$ energies than the UHF geometry, as shown in Table 3. This effect was not so pronounced for the ketone derivative **6**, in which the TCSCF geometry retains PMP-type character with shortened exocyclic bonds; but, the CI energy at this geometry lies above that for the UHF geometry. The UHF-SCF and TCSCF levels of theory thus appear inadequate to describe the structure of **5** in a qualitatively appropriate manner.[26] This problem may be due to spin contamination in

(23) Laidler, K. J. *Chemical Kinetics*, 2nd ed.; McGraw-Hill: New York, NY, 1965; pp 19−21.

(24) Langhoff, S. R.; Davidson, E. R. *Int. J. Quantum Chem.* **1974**, *8*, 61.

(25) Kato, S.; Morokuma, K.; Feller, D.; Davidson, E. R.; Borden, W. T. *J. Am. Chem. Soc.* **1983**, *105*, 1791.

(26) Borden, W. T.; Davidson, E. R.; Feller, D. *Tetrahedron* **1982**, *18*, 737.

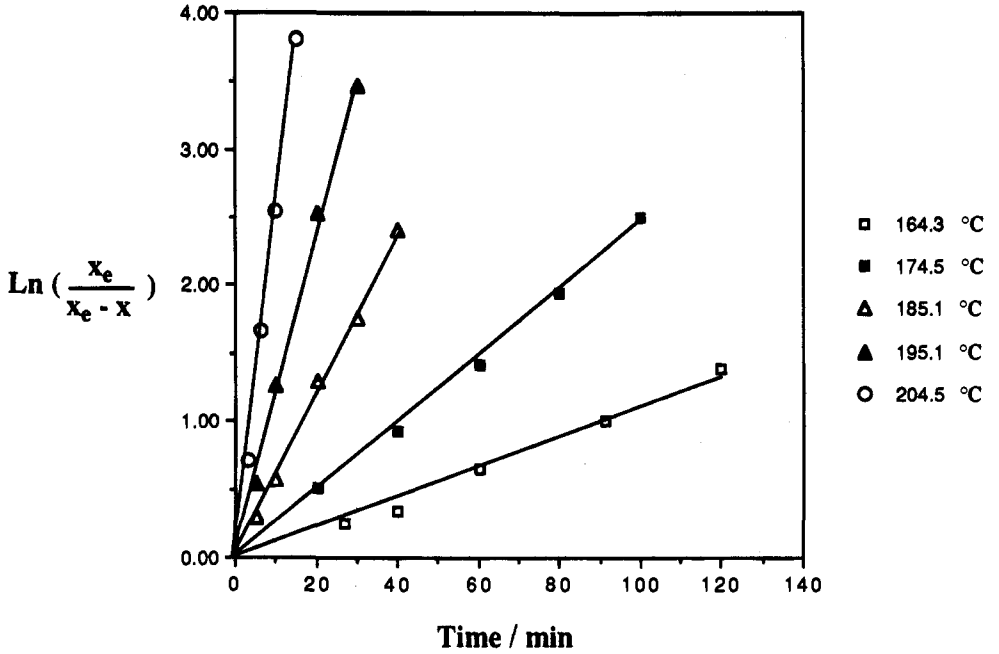

Figure 3. Omnibus plot for epimerizations of *endo*-**7** as a function of time (min) at various temperatures shown in the legend. The definition of concentration variable x is given in the text.

Table 2. Ab Initio Computed $^3B_2$ and $^1A_1$ Energies for **5** and **6** at Different Levels of Theory Using a 6-31G* $^3B_2$ UHF Geometry

computational level	$^3B_2$ energy[a]	$^1A_1$ energy[a]	ΔE[b]	no. of SACs ($^3B_2$, $^1A_1$)[c]
		5		
RHF/TCSCF[d]	−346.493 64	−346.492 91	0.5	
π-MRSD[e]	−346.618 68	−346.615 79	1.8	24 193; 13 582
π-MRSDQ[e]	−346.639 31	−346.634 56	3.0	24 193; 13 582
σ,π-MRSD	−346.701 52	−346.699 47	1.3	75 386; 38 292
σ,π-MRSDQ	−346.727 09	−346.724 17	1.8	75 386; 38 292
SDTQ(10,12)	−346.587 72	−346.584 56	2.0	32 396; 12 541
		6		
RHF/TCSCF[d]	−382.357 88	−382.357 28	0.4	
σ,π-MRSD	−382.561 88	−382.580 31	1.0	75 386; 38 292
σ,π-MRSDQ	−382.608 10	−382.605 90	1.4	75 386; 38 292
SDTQ(10,12)	−382.450 41	−382.448 05	1.5	32 396; 12 541
SDTQ(20,49)	−382.462 52	−382.459 85	1.7	65 362; 22 847

[a] Energy in hartrees. [b] $\Delta E(^3B_2 - ^1A_1)$ in kcal/mol. [c] Number of spin-adapted configurations (SACs) generated in MELDF for the CI wave functions. [d] ROHF energy for the triplet state, TCSCF energy for the singlet state. σ,π-MRSD calculations done using a single reference configuration for the $^3B_2$ state, two-configuration reference of $2a_2^2 4b_1^0$ and $2a_2^0 4b_1^2$ for the $^1A_1$ state; double excitations were carried out from the full occupied π-space plus the highest three occupied a_1 and highest two occupied b_2 MOs, into a K-orbital subspace of seven a_1, 13 b_1, eight b_2, and eight a_2 MOs. σ,π-MRSDQ energies are MRSD energies with an estimated quadruples correction by the method of ref 24. SDTQ energies were obtained using all 10 p-electrons and the lowest 12 p-MOs (10,12), or using the full π-space, plus the highest three occupied a_1 and highest two occupied b_2 MOs, exciting at the quadruples level into the lowest 37 virtual K-orbitals (10,49). [e] π-MRSD calculations done as described in d, but using a π-only orbital subspace for double excitations.

the UHF-SCF wave function, as shown by the fact that $\langle S^2 \rangle$ = 2.93 and 2.66 before annihilation (2.51 and 2.26 after) for **5** and **6**, respectively.

We carried out point-by-point partial CI optimization of PMP **5** by varying first the central C=CH_2 bond, and then the connector C_2—C_3 (C_3—C_4) bonds at the SDTQ-CI 6-31G* level, and obtaining both $^1A_1$ and $^3B_2$ energies at each fixed geometry. The optimal central C=CH_2 bond is substantially shorter and more localized at the post-Hartree−Fock level (1.342 Å) than at the UHF-SCF level (1.376 Å). In addition, the connecting C—C bond lengthens from 1.477 to 1.496 Å. For **6**, a similar but lesser trend is observed, with the C=O bond shortening from 1.214 to 1.204 Å and the C—C bond lengthening from 1.487 to 1.497 Å. For **5**, the CI-optimized PMP-type structure for the $^1A_1$ state is lower in energy than the localized TCSCF structure. Overall, virtually no difference between the optimal $^3B_2$ and $^1A_1$ geometries was found for either **5** and **6** and the $^1A_1$ state remained higher in energy than the $^3B_2$ state at any given fixed geometry.[27] Table 2 contains energies and CI active space descriptions for PMPs **5** and **6** at various levels of theory attempted by us.

Qualitatively, the $^3B_2$ and $^1A_1$ states of both **5** and **6** prefer structures consisting of delocalized allyl groups weakly connected through their inactive central sites by cross-conjugating >C=CH_2 or >C=O linker groups. The central >C=CH_2 and >C=O have bond lengths consistent with localized, rather than partly conjugated, double bonds, in agreement with the disjoint nature of PMPs. Electronic communication between the allyl fragments of the PMP is so limited that substantial geometric differentiation between triplet and singlet states is not energetically favorable.

Computational Analysis of PMP Electronic Structure. Analysis of the SDTQ-CI wave functions for **5** and **6** shows the diradical nature of PMP. The $^3B_2$ states in both systems, of course, are diradicals. The $^1A_1$ states, rather than being closed shell, also are diradical in nature. The squared ratio of the two major CI coefficients, c_1^2/c_1^2 should be nearly unity for a diradical singlet CI wave function.[6] In addition, the occupancy numbers of the two frontier natural orbitals (NOs) of a diradical state should both be nearly 1, while those of a closed shell system will all be nearly 2 or 0. π-SDTQ-CI coefficients and NO occupancy data for the states of **5** and **6** are compiled in Table 4. The NO results show populations for the b_1 and a_2 singly occupied MOs (SOMOs). All data show the PMP $^1A_1$ states to be diradical in nature.

The spin density distribution of the $^3B_2$ states indicates some perturbation of the PMP p-system by the methylene sp^3 group that constrains planarity in **5** and **6**. Most of the spin density

(27) Prof. W. T. Borden has also found in independent calculations that PMPs appear to prefer a $^3B_2$ ground state by a small energetic margin (Borden, W. T. Private communication). We thank Prof. Borden for sharing this result with us.

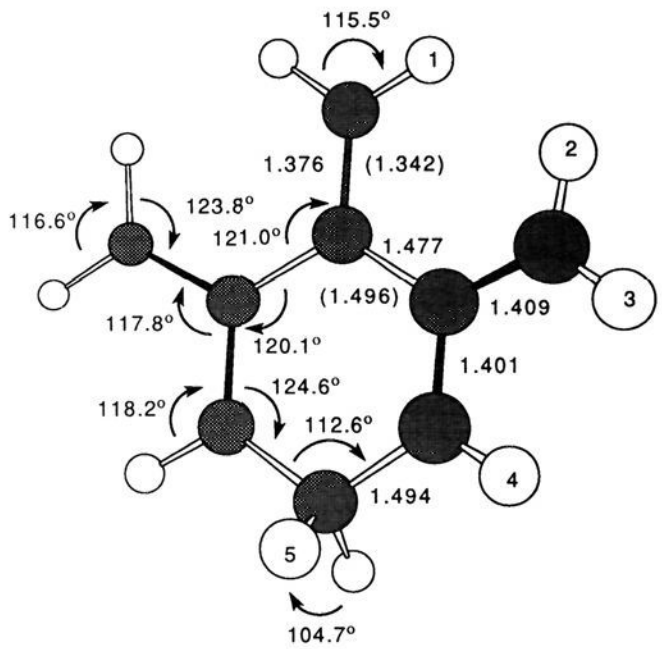

r C-H$_1$ = 1.071
r C-H$_2$ = 1.071
r C-H$_3$ = 1.074
r C-H$_4$ = 1.076
r C-H$_5$ = 1.092

5 ($^3B_2$ UHF)

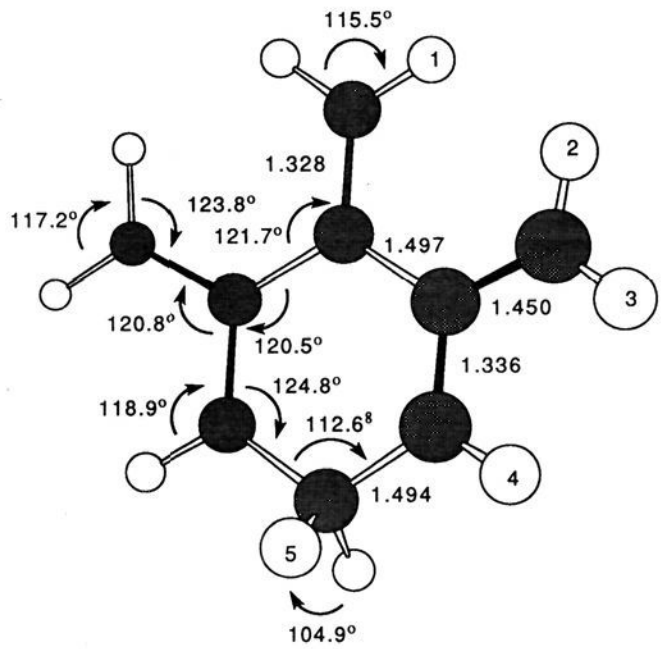

r C-H$_1$ = 1.071
r C-H$_2$ = 1.071
r C-H$_3$ = 1.073
r C-H$_4$ = 1.077
r C-H$_5$ = 1.091

5 ($^1A_1$ TCSCF)

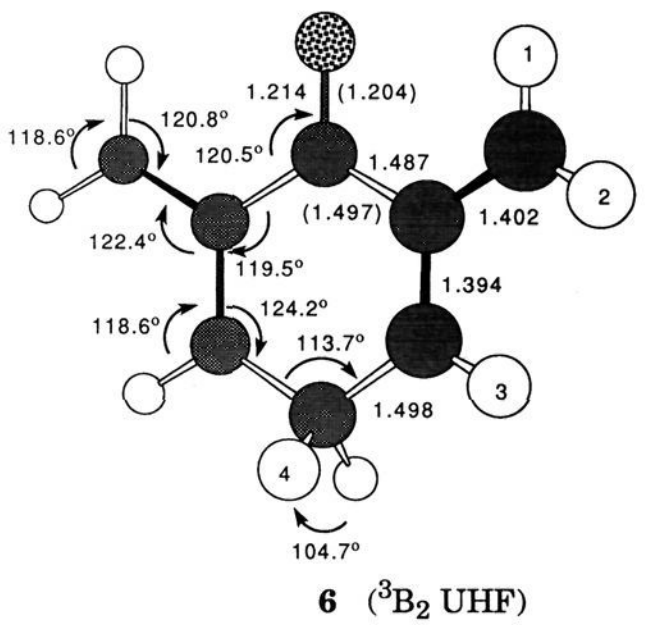

r C-H$_1$ = 1.071
r C-H$_2$ = 1.074
r C-H$_3$ = 1.076
r C-H$_4$ = 1.092

6 ($^3B_2$ UHF)

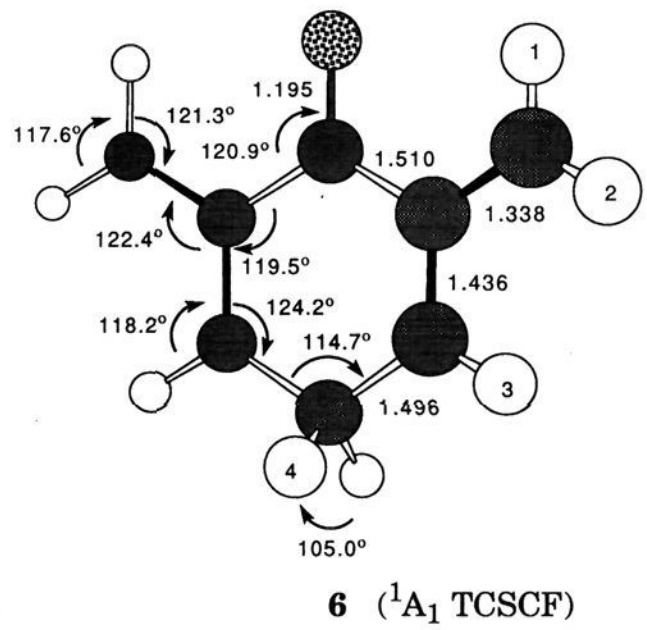

r C-H$_1$ = 1.072
r C-H$_2$ = 1.075
r C-H$_3$ = 1.075
r C-H$_4$ = 1.091

6 ($^1A_1$ TCSCF)

Figure 4. Computed geometric parameters for PMPs **5** and **6**, using the $^3B_2$ 6-31G* UHF wave functions; partially optimized 6-31G* SDTQ-CI values for the >C=CH$_2$ and C(sp^2)—C(sp^2) bonds are shown on the same structure in parentheses. $^1A_1$ 6-31G* TCSCF optimized values are shown for **5** and **6** in brackets on separate structures. Bond lengths are in angstroms, bond angles in degrees.

Table 3. Ab Initio 6-31G* SDTQ-CI Energies for **5** and **6** at Various Geometries

geometry	$^3B_2$ energy[a]	$^1A_1$ energy[a]	ΔE[b]
	5		
$^3B_2$ UHF	−346.587 72	−346.584 56	2.0
$^1A_1$ TCSCF	−346.588 34	−346.585 89	1.5
SDTQ-CI	−346.589 22	−346.586 36	1.8
	6		
$^3B_2$ UHF	−382.450 41	−382.448 05	1.5
$^1A_1$ TCSCF	−382.442 85		
SDTQ-CI	−382.450 81	−382.448 56	1.4

[a] Energy in hartrees at UHF, TCSCF and partially optimized SDTQ-CI geometries. At each fixed geometry (see Figure 4), both $^3B_2$ and $^1A_1$ states were computed, using SDTQ-CI with a 10 electron, 12 π-MO active space (including all occupied π-MOs). [b] $\Delta E(^3B_2-{}^1A_1)$ in kcal/mol for states at the same geometry.

Table 4. Comparison of CI Coefficients and Natural Orbital Occupancies of the Two Leading Configurations in the Singlet CI Wave Functions of **5** and **6**

				NO occupancy[b]	
computation	C_1[a]	C_2[a]	C_1^2/C_2^2	$4b_1$	$2a_2$
		5			
SDTQ(π)[c]	0.651	0.651	1.001	0.998	1.003
σ,π-MRSD[d]	0.664	0.662	1.006	0.997	1.003
		6			
SDTQ(π)[c]	0.670	0.643	1.084	0.959	1.042
σ,π-MRSD[d]	0.679	0.652	1.084	0.959	1.037

[a] Largest $^1A_1$ state CI wave function coefficients (C_1 for the π-configuration having $2a_2^2 4b_1^0$, C_2 for the configuration having $2a_2^0 4b_1^2$). [b] MELDF $^1A_1$ state natural orbital (NO) occupancy number for each CI wave function. [c] SDTQ CI wave function with 10 electrons and 12 π-MOs using the scheme described in Table 3. [d] σ,π-MRSD-CI wave functions using the scheme described in Table 3.

in both systems lies on the termini of the allylic groups (Figure 5), with small spin-polarized populations being computed at the central allylic carbons and virtually no spin density at the central linker groups >C=CH$_2$ and >C=O. The difference in spin densities between the terminal carbons of each allyl fragment in the PMPs **5** and **6** is consistent with a slight asymmetry in the allylic C—C bond lengths.

We considered the possibility that the allyl fragment asymmetry might be due to an electronic perturbing effect of the sp^3 methylene group. To check this, we optimized the structure of parent PMP **2** at the UHF-SCF 6-31G* level of theory with a planar C_{2v} constraint. With all other bonding parameters fixed, we varied the central C=CH$_2$ bond length from the UHF value of 1.384 Å and carried out 6-31G* p-SDTQ-CI fixed point computations to improve this parameter. We estimated the optimum C=CH$_2$ bond length under these constraints to be 1.340 Å. Since the $^3B_2$ and $^1A_1$ states for cyclic PMP **5** had similar geometries, we assumed the same geometry for both the $^3B_2$ and $^1A_1$ states of **2** and carried out fixed point π-SDTQ-CI 6-31G* computations. The energy and geometric results of these computations are summarized in Figure 6 and Table 5.

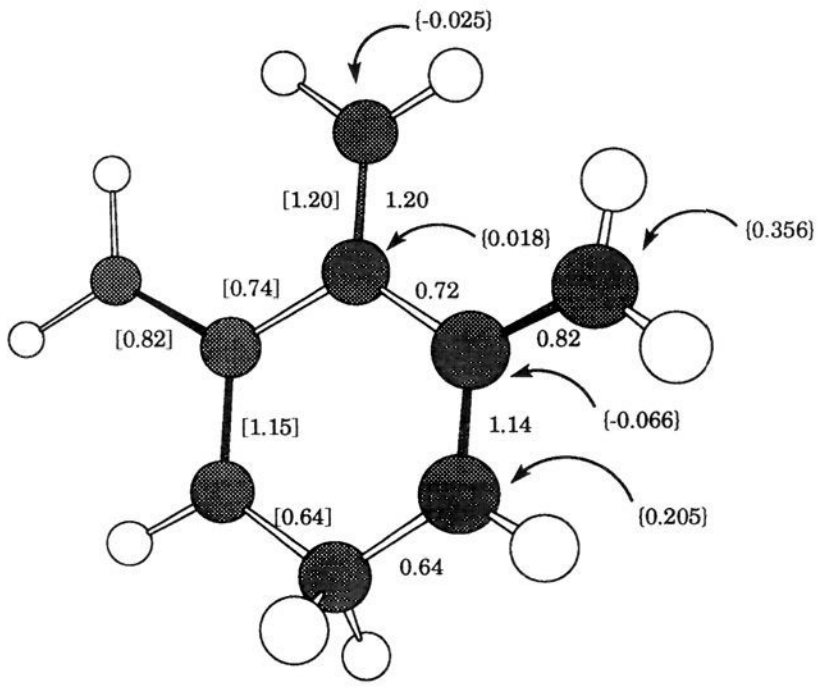

5

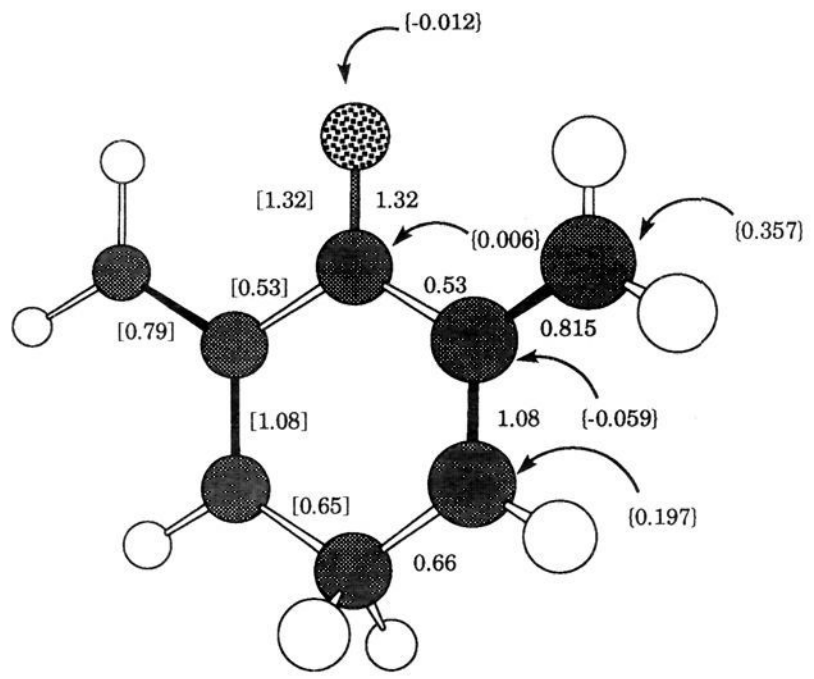

6

Figure 5. SDTQ-CI 6-31G* [bond orders] for the $^1A_1$ states of **5** and **6**; bond orders and {spin populations} for the $^3B_2$ states of **5** and **6**.

We found that PMP **2** is geometrically well-described as 1,1-bis(2-allyl)ethene, analogously to the constrained system **5**. As in the cyclic analogues, the central C=CH_2 bond length is substantially shorter at the SDTQ-CI level of theory than at the UHF triplet level, again due presumably to spin contamination in the UHF 6-31G* wave function ($\langle S^2\rangle = 2.971$, $\langle S^2\rangle_{annih} = 2.575$). The π-SDTQ-CI $\Delta E(T - S) = 1.4$ kcal/mol, very similar to the gap found for **5** and **6**. Natural orbital analysis for the $^1A_1$ state of **2** shows the population numbers for the b_1 and a_2 NOs to be 1.047 and 0.953 at the SDTQ-CI level, showing a diradical electronic nature that is very similar to that for **5**. The geometry and electronic nature for PMP thus appear to be little effected by the methylene bridging in **5** and **6**.

Figure 6 also shows the bond order and spin population distribution obtained from the SDTQ-CI wave function by MELDF for **2**. There is some asymmetry in the bond order and spin distribution, which is similar to the slight asymmetry that is found for the allyl fragment bond lengths in **2**. The allyl C−CH_2 units that are *syn* to the central linker unit are slightly longer, and slightly less strongly bonded, than those which are *anti*. The resultant bond and spin populations for **2** turn out to be very similar to those for the cyclic PMP **5**. As a result, we feel that the electronic effect of the methylene group on the

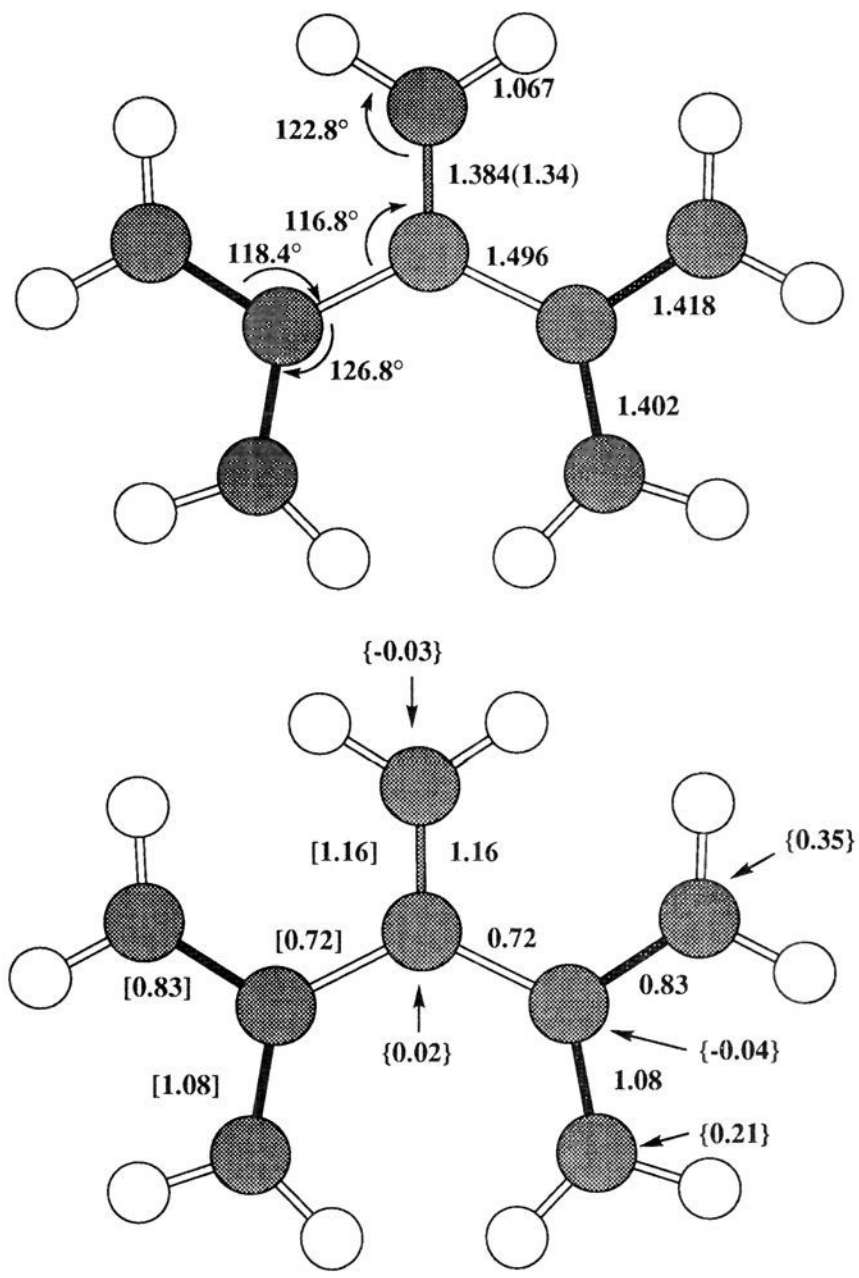

Figure 6. Computed geometric parameters for PMP (**2**) $^3B_2$ 6-31G* UHF wave function (6-31G* SDTQ-CI-optimized value of the C=CH_2 bond is in parentheses). Computed 6-31G* SDTQ-CI [bond orders] for the $^1A_1$ state; bond orders and {spin densities} for the $^3B_2$ state.

Table 5. Ab Initio 6-31G* SDTQ-CI Energies for PMP (**2**)

geometry	$^3B_2$ energy[a]	$^1A_1$ energy[a]	ΔE[b]
$^3B_2$ UHF	−308.675 66	−308.673 23	1.5
part. SDTQ-CI	−308.676 97	−308.674 73	1.4

[a] Energy in hartrees using both a $^3B_2$ UHF geometry and a partially SDTQ-CI-optimized one with r(C=CH_2) = 1.340 Å. All computations carried out at a single fixed geometry for both $^3B_2$ and $^1A_1$ states, using SDTQ-CI with an 8 electron, 11 π-MO active space. [b] $\Delta E(^3B_2 - ^1A_1)$ in kcal/mol at each fixed geometry.

computations for **5** is of minimal importance and that PMPs related to **5** and **6** are good experimental targets, since they should be minimally perturbed models for the parent system **2**.

Overview of Computational Results. Overall, the PMPs computationally are found to have the general electronic structural characteristics predicted by Borden and Davidson. These disjoint systems have quite small triplet−singlet gaps which are not greatly changed by the exact nature of the central linking group (>C=CH_2 versus >C=O) and are best described as being very weakly linked "bis(allyl)"-type systems in terms of their electronic structure. Gross geometric differences between the $^3B_2$ and $^1A_1$ states of the cyclically constrained PMPs are not expected due to the weak linkage between the allyl moieties and were not found, nor did $\Delta E(T - S)$ vary appreciably as a function of geometry.

Discussion

Intrinsic Ground State Multiplicity of PMPs. In their ground-breaking work describing the disjoint class of π-con-

Chart 5

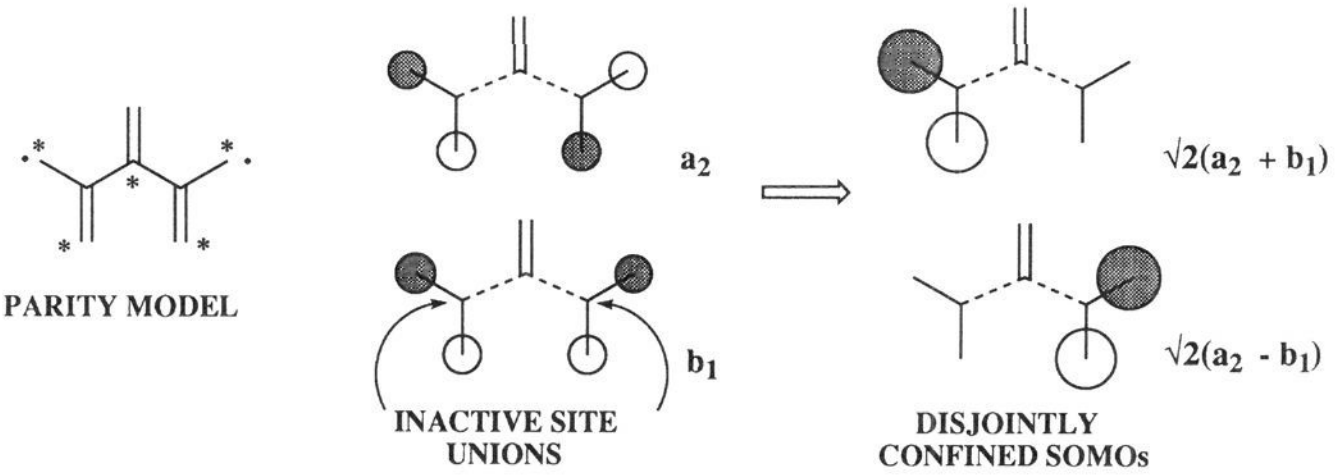

jugated diradicals, Borden and Davidson pointed out that PMP (**2**) is an example of a system that is disjoint, despite the fact that parity-based models would predict it to have a high-spin ground state. For instance, use of the Ovchinnikov[28,29] or Klein[30−32] models yields $n^* = 5$ and $n^0 = 3$, hence a triplet ground state is expected for a planar system. However, the fact that PMP (**2**) may be dissected into discrete allyl units—joined by a 1,1-ethenediyl linker unit at inactive sites—allows the unpaired electrons in PMP to be localized in the separate allyl portions of the molecule. In an alternate formulation of the same idea, by appropriate linear combination of the the symmetrized b_1 and a_2 SOMOs of **2**, one may obtain a pair of localized SOMOs of zero atomic overlap, such that interaction between electrons in these SOMOs is very small. The manner in which such disjointly nonoverlapping orbitals leads to very small $\Delta E(T - S)$ has been previously described by Borden[1] and Davidson.[2]

Qualitatively, a discrepancy has often been perceived between the disjoint and the parity-based descriptions of PMP (**2**) and related molecules. Borden and Davidson[2] pointed out that disjoint systems might very well prefer to have singlet ground states, due to the limited effect of exchange between unpaired electrons is such molecules. However, whatever the actual ground state spin multiplicity of a disjoint system, it is clear that $\Delta E(T - S)$ will be quite small in such cases, such that small geometric or substituent-related factors may tilt the balance toward either high- or low-spin multiplicity in any given system.

The story of TME (**1**) has proved an excellent example of this caveat to the disjointness classification scheme. TME was pointed out by Borden and Davidson as an archetypal disjoint system, which is also expected by parity-based models to have a singlet ground state. But, experimental electron spin resonance studies by Dowd and co-workers[3] indicated that TME is a ground state triplet molecule. Various computational investigations were at odds with this finding, and obtained singlet ground state preferences by gradually decreasing predicted margins, until the most recently published study by Nachtigall and Jordan[8] found—after a strenuous search at fairly substantial levels of theory of the conformations available to TME—that a triplet GS can be computationally obtained for TME (**1**). $\Delta E(T - S)$ for **1** is predicted to be only 1.0−1.5 kcal/mol. The actual ground state is dependent on the dihedral angle between the allyl fragments across the central C—C bond in this very weakly

(28) Misurkin, I. A.; Ovchinnikov, A. A. *Russ. Chem. Res. (Engl).* **1977**, *46*, 967.
(29) Ovchinnikov, A. A. *Theor. Chim. Acta* **1978**, *47*, 297.
(30) Klein, D. J.; Nelin, C. J.; Alexander, S.; Matsen, F. E. *J. Chem. Phys.* **1982**, *77*, 3101.
(31) Klein, D. J. *Pure Appl. Chem.* **1983**, *55*, 299.
(32) Klein, D. J.; Alexander, S. A. In *Graph Theory and Topology in Chemistry*; King, R. B. and Rouvray, D. H., Eds.; Elsevier: Amsterdam, The Netherlands, 1987; Vol. 51; p 404.

Chart 6

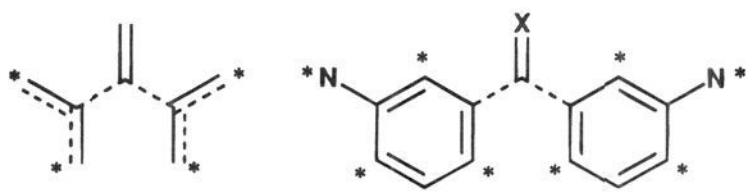

2 **3**

exchange coupled diradical. This demonstrates how the qualitative prediction of a small energy gap between singlet and triplet states in disjoint systems should not be mistaken for an absolute rule predicting a low-spin ground state, when small and possibly opposing effects can be so important in determining the actual ground state spin multiplicity.

Shortly after publication of our preliminary communication describing some of the experimental results presented in this paper,[13] our group[11] and that of Iwamura[12] simultaneously published electron spin resonance Curie law studies of the quintet states of dinitrene molecules **3** shown earlier. Both the ethenediyl- and carbonyl-linked variants of **3** were found to have low-spin ground states by small energetic margins, with the observable ESR-active quintets being thermally populated excited states. Iwamura described this class as being doubly disjoint.[12] Both papers noted that the dinitrenes **3** are formally related to PMP, since they are composed of spin-bearing moieties that are coupled together by a 1,1-ethenediyl linker unit at inactive sites. The finding of low-spin ground states for **3** is a considerable victory for the disjointness criterion, since parity-based models would predict structure **3** to lead to high-spin ground states. Recently, we have also found that a planar constrained analogue of **3** has a low spin-ground state,[33] suggesting the conformational effects in **3** are not solely responsible for its low-spin ground state.

Our computational results described above suggest a small preference for a triplet ground state for PMPs **2**, **5**, and **6**, in accord with the spin polarization arguments that govern the parity-based models for conjugated diradicals. The preference is small enough that minor effects of geometric distortion or substitution pattern might cause a singlet to be favored in any given case. As a result, we must content ourselves with noting that the qualitative similarity of singlet and triplet states in all the PMP computations is in accord with the disjoint description of these systems.

Experimental Support for Intermediacy of PMPs. The one previously published study for which PMP intermediacy has been suggested was the work of Kaupp and Zimmerman.[34] These workers showed that solid state photolysis of 2,5-

(33) Ling, C.; Lahti, P. M. *Chem. Lett.* **1994**, 1352, 2447.
(34) Kaupp, G.; Zimmerman, I. *Angew. Chem., Int. Ed. Engl.* **1981**, *20*, 1018.

Chart 7

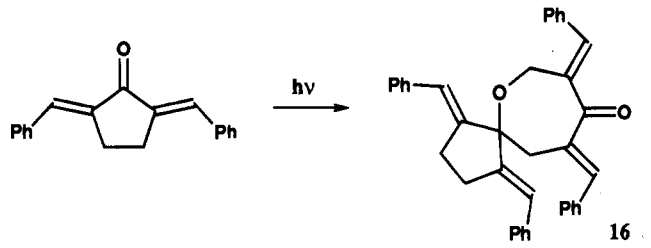

16

dibenzylidenecyclopentanone gave dimeric product **16**, among other products. This compound is consistent with addition of a PMP-type intermediate across the carbonyl bond of the starting material. No direct evidence was described in this report to support formation of a discrete PMP in this process.

Our experiments in frozen solution matrix showed no photoisomerization of precursors **7** or **15**, precluding the formation of a PMP intermediate or transition state under these circumstances. This may be due to an inability of **7** to planarize in the matrix cage (or in the neat solid state). Alternatively, the facile frozen solution fluorescence and phosphorescence that we observed in these systems may not allow a sufficient excited state lifetime for planarization to occur under these circumstances. Compound **15** and its analogues in particular showed strong fluorescence and phosphorescence. In the solution phase, the relative rates of photolytic cleavage and photoluminescence are apparently appropriate to allow planarization, unless one assumes that all of the photoisomerization proceeds through the side-bond cleavage (*vide supra*). Picosecond laser UV−vis spectroscopy showed[35] apparent formation of singlet and triplet excited states of the ketone **4** in dichloromethane at room temperature but no evidence for a PMP intermediate. Photoisomerization of bicycloketones **4**, **7**, **14**, and **15** therefore is inconclusive with regard to providing definitive evidence for the generation of PMPs.

The thermal experiments are more supportive of PMP generation, although direct observation of PMPs was not possible. Our best evidence comes from a comparison of the Eyring parameters for thermal isomerization of **7** to those of some previously studied systems. Table 6 shows a number of literature comparisons.

By comparison to those for the thermolyses of 2-methylvinylcyclopropane and vinylcyclopropane, the Arrhenius parameters for isomerization of **7** show a substantially lower activation barrier and lower *A*-value. However, the comparison to the isomerization barrier for *trans*-1,2-divinylcyclopropane—which will proceed via cyclopropane ring rupture—is very similar. The slightly lower value for **7** is probably attributable in part to stabilizing influence of the exocyclic phenyl substituents upon a diradical intermediate or diradicaloid transition state. The low Arrhenius *A*-value and negative Eyring $\Delta S^{\ddagger}$ show a substantial degree of ordering in the transition state for epimerization of **7**, consistent with a transition state in which phenyl-group resonance stabilization would be enhanced by coplanarity of these rings with the rest of a PMP-type conjugated system. The isomerization of bicyclo[3.1.0]hexane has an activation barrier of >57 kcal/mol without the benefit of conjugation. The addition of each vinyl group to a cyclopropane ring lowers E_a for isomerization by about 15−16 kcal/mol in the series cyclopropane, vinylcyclopropane, 1,2-divinylcyclopropane. By analogy, placement of two vinyl groups on a bicyclohexane to make **7** should lower the E_a of cleavage of the central bond by about 30 kcal/mol to about 27−30 kcal/mol. This is just what is observed.

(35) We thank the research group of Prof. E. Hilinski for performing this experiment for us (Mecklenburg, S.; Hilinski, E. F. Unpublished results, private communication, 1989). The picosecond laser setup was described in the following: Schmidt, J. A.; Hilinski, E. F. *Rev. Sci. Instrum.* **1989**, *60*, 2902.

Table 6. Arrhenius Parameters for Some Cyclopropane Ring-Opening Reactions

REACTION	log A	E_{act}
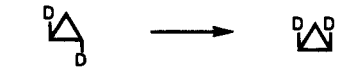	16.4	65.1 [a]
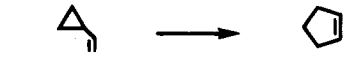	13.5	49.6 [b]
	14.8	48.6 [c]
	13.1	34.3 [d]
	13.3	57.4 [e]
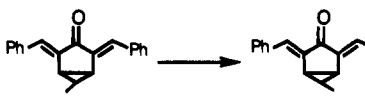	11.2	31.0

[a] Rabinovitch, B. S.; Schlag, E. W. *J. Am. Chem. Soc.* **1960**, *82*, 5996. [b] Flowers, M. C.; Frey, H. M. *J. Chem. Soc.* **1964**, 3547. [c] Ellis, R. J.; Frey, H. M. *J. Chem. Soc.* **1964**, 5578. [d] Arai, M.; Crawford, R. *J. Can. J. Chem.* **1972**, *50*, 2158. [e] Frey, H. M.; Smith, R. C. *Trans. Faraday Soc.* **1962**, *58*, 697.

Chart 8

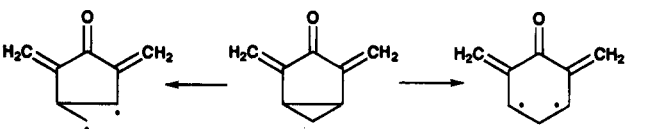

17 13 6

A thermochemical group equivalent estimation of the relative heats of formation for PMP **6** and its associated bicyclic precursor **13** also shows that the PMP is a reasonable intermediate in the epimerization of **7** (see the supplementary material). PMP **6** is estimated to lie about 22−27 kcal/mol above bicyclic **13**, in reasonable agreement with the experimental value of 29 kcal/mol for $\Delta H^{\ddagger}$ in epimerization of **7**. The side-bond cleaved diradical **17**—which has only one radical center stabilized by a neighboring vinyl group—lies considerably higher in energy than **6**. This is consistent with the observation that *cis*−*trans* isomerization of vinylcyclopropanes is 15 kcal/mol more difficult than the corresponding isomerization of 1,2-divinylcyclopropanes (Table 6, *vide supra*). Naturally, the group equivalent method of modeling the intermediacy of diradicals is subject to various possible uncertainties. For example, we have no proof that the planarizing structure in the epimerization of **7** is an energy minimum—it may simply be a transition state, which would not be experimentally observable. Still, the good agreement of the computationally predicted nature of PMP **6** with the experimental results supports the presence of PMPs as intermediates or transition states in the epimerization of **7**.

Overall, we did not obtain direct evidence for the formation of PMP intermediates. However, we believe the accumulation of indirect evidence for a very short-lived PMP intermediate or a PMP-type transition state in the isomerization of **7** to be convincing, especially for the thermal process. We attribute the elusiveness of the PMPs themselves in these reactions to a

combination of unfavorable photochemistry in rigid media, and facile ring closure to the original precursors in solution phase media.

Conclusion

We have shown computationally that PMPs are expected to have at most a small preference for a triplet high-spin ground state, as expected by the Borden/Davidson disjointness criterion. This is roughly in agreement with experimental findings for PMP-like "doubly-disjoint" dinitrene systems, but different in that the dinitrenes have singlet ground states with very low lying high-spin states. It is possible that heteroatom substitution or minor geometric factors may alter the ground state spin preference in the dinitrene analogues, relative to the structurally simpler PMPs.

Experimental attempts to generate a constrained PMP from a bicyclic precursor gave no direct evidence for a triplet PMP but were consistent with PMP generation as a transient intermediate or transition state that forms during solution phase isomerization of the precursor. The elusiveness of the putative PMPs in cryogenic studies appears to be due to competing photochemical pathways available to the bicyclic PMP precursors under rigid phase conditions.

Experimental Section

2,4-Dibenzylidenebicyclo[3.1.0]hexan-3-one (4). A 100 mL round-bottom flask was charged with ketone **10** (0.01 mol, 1.0 g), benzaldehyde (0.03 mol, 3.2 g), sodium hydroxide (0.03 mol, 1.2 g), ethanol (20 mL), and water (20 mL). The reaction was stirred at room temperature for 1 h. The solution was cooled in an ice bath and the yellow solid collected. Recrystallization from ethanol/water gave 1.1 g (40%) of **4** as yellow needles, mp 166−167 °C. Anal. Calcd for $C_{20}H_{16}O$: C, 88.19; H, 5.93; O, 5.87. Found: C, 87.99; H, 5.77. ^{1}H NMR (300 MHz): δ 7.18−7.94 (m, 12H, vinyl and phenyl), 2.73 (dd, J = 4.2, J = 7.9, 2H, bridge CH), 1.84 (m, 1H, *exo* cyclopropyl), 1.00 (m, 1H, *endo* cyclopropyl). IR (KBr, cm^{-1}): 3028 (w), 3019 (w), 2360 (w), 1697 (C=O), 1630 (vs), 1617 (vs), 1259, 1188 (vs), 1047, 699.

2,4-Dibenzylidene-*exo*-6-methylbicyclo[3.1.0]hexan-3-one (7). Ketone **11** (0.01 mol, 1.1 g) was reacted with benzaldehyde (0.03 mol, 3.2 g) in the same manner as **10**. Recrystallization of the yellow solid from ethanol/water afforded 0.76 g (48% yield) of **7** as yellow needles, mp 171−172 °C. Anal. Calcd for $C_{21}H_{18}O$: C, 88.07; H, 6.35; O, 5.59. Found: C, 87.92; H, 6.67. ^{1}H NMR (300 MHz, C_6D_6): δ 7.92 (s, 2 H, vinyl =CH), 7.21−7.62 (m, 10 H, phenyl), 2.06 (d, J = 3.4 Hz, 2H, bridge CH), 0.95 (d, J = 6.1 Hz, 3H, CH_3), 0.80 (m, 1 H, J = 3.4 Hz, J' = 6.1 Hz, endo C_6-H). IR (KBr, cm^{-1}): 3025 (w), 2951 (w), 2371 (w), 1701 (C=O), 1632 (vs), 1618 (vs), 1260, 1185 (vs), 1045 (vs).

***exo*-6-Methylbicyclo[3.1.0]hexan-3-one-*2,2,4,4-d*$_4$ (11-*2,2,4,4-d*$_4$).** A 50 mL round-bottom flask was charged with ketone **11** (0.02 mol, 2.2 g) and methanol-*O-d* (15 mL). A crumb of sodium (rinsed with pentane) was added and the reaction allowed to stir for 3 h. The methanol-*O-d* was removed under vacuum and the residue diluted with 20 mL of deuterium oxide, extracted with ether, and worked up as described for **11** above. This procedure was repeated two times until the α-protons were no longer present by ^{1}H NMR. Bulb-to-bulb distillation afforded 0.20 g (9%) of **11**-*2,2,4,4-d*$_4$ as a clear liquid. ^{1}H NMR (80 MHz): δ 1.20 (d, J = 3.3 Hz, 2 H, bridge), 1.02 (d, J = 6.0 Hz, 3 H, methyl), 0.20 (m, 1 H, J = 6.0 Hz, J' = 3.3 Hz, cyclopropyl CH).

2-Benzylidene-*exo*-6-Methylbicyclo[3.1.0]hexan-3-one (12). Sodium hydroxide (0.02 mol, 0.8 g) dissolved in water (20 mL), ketone **11** (0.026 mol, 2.86 g), and benzaldehyde (0.013 mol, 1.38 g) were stirred at room temperature for 45 min. Concentrated HCl (15 mL) was then added to the orange reaction mixture. The reaction mixture was then extracted with ether (4 × 50 mL), the combined organic layers were washed with saturated sodium bisulfite ($NaHSO_3$) (20 mL), and the mixture was worked up in the usual manner. Distillation gave 0.33 g (13%) of **12**, bp 110−124 °C (0.5 mm Hg), as a yellow oil. Recrystallization from hexane afforded slightly yellow crystals, mp 61−63 °C. Anal. Calcd for $C_{14}H_{14}O$: C, 84.80; H, 7.13; O, 8.07. Found: C, 85.40; H, 7.28. ^{1}H NMR (300 MHz): δ 7.18−7.81 (m, 6 H, phenyl and vinyl), 2.67 (dd, J = 6.4, J' = 19.6, 1 H, −CH−H), 2.40 (d, J = 19.6, 1 H, −CH−H), 2.22 (dd, J = 2.8, J' = 6.7, 1 H, H_c), 1.56 (ddd, J = 6.7, J' = 6.4, J'' = 3.8, 1 H, H_b), 1.30 (d, J = 6.1, 3 H, CH_3), 0.82 (m, 1 H, *endo* cyclopropyl CH). IR (KBr, cm^{-1}): 3039 (w), 3010 (w), 2941, 2919 (m), 2351 (w), 1709 (vs, C=O), 1641 (vs), 1255, 1227, 1181 (vs), 753, 701.

2,4-Bis[(*N,N*-dimethylamino)methylene]bicyclo[3.1.0]hexan-3-one (14). A 25 mL round-bottom flask was charged with ketone **10** (0.006 mol, 0.58 g) and freshly distilled *N,N*-dimethylformamide di-*tert*-butyl acetal (0.015 mol, 3.1 g), purchased from Lancaster Synthesis, Ltd. The reaction was heated at 90 °C for 24 h, after which the reaction was cooled and a distilling head attached. The reaction was again heated to 90 °C and *t*-BuOH(5 mL) distilled over. The reaction was cooled to room temperature and all volatiles were removed under reduced pressure. The resulting orange-brown solid was recrysallized twice from ether to give 0.17 g (14% yield) of **14** as orange needles, mp 167−169 °C. Anal. Calcd for $C_{12}H_{18}N_2O$: C, 69.85; H, 8.81; N, 13.58; O, 7.75. Found: C, 69.95; H, 8.86; N, 13.67. ^{1}H NMR (300 MHz): δ 7.07 (s, 2H, =CH), 3.11 (s, 12H, $N(CH_3)_2$), 2.30 (m, 2H, bridgehead CH), 1.03 (m, 1H, exo cyclopropyl CH), 0.41 (m, 1H, *endo* cyclopropyl CH). UV−vis (EtOH): 388 nm (49 000 M^{-1} cm^{-1}). Fluorescence (EtOH, λ_{excit} = 360 nm): 427 nm (Φ = 0.0058). Phosphorescence (EtOH, 77 K, λ_{excit} = 360 nm): 538 nm. IR (KBr, cm^{-1}): 2990 (m), 2370 (w), 1615 (vs, C=O), 1562.

2,4-Bis[(*N,N*-dimethylamino)methylene]-*exo*-6-methylbicyclo-[3.1.0]hexan-3-one (15). Ketone **11** (0.009 mol, 1.0 g) and freshly distilled *N,N*-dimethylformamide di-*tert*-butyl acetal (0.022 mol, 4.5 g) were reacted in the same manner as was used to make **14**. The resulting brown solid was recrystallized from ether to give 0.27 g (14% yield) of **15** as orange needles, mp 124−125 °C. Anal. Calcd for $C_{13}H_{20}N_2O$: C, 70.86; H, 9.17; N, 12.72; O, 7.26. Found: C, 70.83; H, 9.22; N, 12.73. ^{1}H NMR (300 MHz): δ 7.04 (s, 2H, =CH), 3.10 (s, 12H, $N(CH_3)_2$), 1.98 (d, J = 3.2, 2H, bridgehead CH), 1.09 (d, J = 6.1, 3H, CH_3), 0.70 (m, 1H, *endo* cyclopropyl CH). UV-vis (EtOH): 392 nm (43 000 M^{-1} cm^{-1}). Fluorescence (EtOH, λ_{excit} = 360 nm): 430 nm (Φ = 0.0039). Phosphorescence (EtOH, 77 K, λ_{excit} = 360 nm): 550 nm. IR (KBr, cm^{-1}): 2916 (m), 1610 (vs, C=O), 1562.

Acknowledgment. We acknowledge support from the Donors of the Petroleum Research Fund, administered by the American Chemical Society (PRF 21150-AC4). Partial support came from grants by the National Science Foundation (CHE 8712319 and 9204695). We also acknowledge a grant of computer time by the Cornell National Supercomputer Center, a resource of the Center for Theory and Simulation in Science and Engineering (Theory Center), which receives major funding from the National Science Foundation and the IBM Corp., with additional support from New York State and members of the Corporate Research Institute. We are grateful to Professor Weston T. Borden for helpful and encouraging discussions of this work.

Supplementary Material Available: Text describing general procedures, spectroscopy, and characterization methods. Synthesis and characterization of 1-hydroxy-dicyclopentadiene, 3-cyclopenten-1-one, 3-cyclopenten-1-ol, and compounds **8**−**11**. Experimental methodology for kinetic runs summarized in Table 1. Figure S1 showing thermochemical analysis of **6**, **13**, and **17**. (Total of 6 pages). This material is contained in many libraries on microfiche, immediately follows this article in the microfilm version of the journal, can be ordered from the ACS, and can be downloaded from the Internet; see any current masthead page for ordering information and Internet access instructions.

JA950007U